Electronic Supplementary Information for:

Intrinsic Helical Twist and Chirality in Ultrathin Tellurium Nanowires

*Alejandra Londoño-Calderon,[a] Darrick J. Williams,[a] Matthew M. Schneider,[b] Benjamin H. Savitzky,[c] Colin Ophus,[c] Sijie Ma,[d] Hanyu Zhu,[d] and Michael T. Pettes[a,]**

[a] Center for Integrated Nanotechnologies, Materials Physics and Applications Division, Los Alamos National Laboratory, Los Alamos, New Mexico 87545, USA

[b] Materials Science in Radiation and Dynamics Extremes (MST-8), Materials Science and Technology Division, Los Alamos National Laboratory, Los Alamos, New Mexico 87545, USA

[c] NCEM, Molecular Foundry, Lawrence Berkeley National Laboratory, Berkeley, California 94720, USA

[d] Department of Materials Science and NanoEngineering, Rice University, Houston, Texas 77005, USA

* Corresponding author, Email: pettesmt@lanl.gov

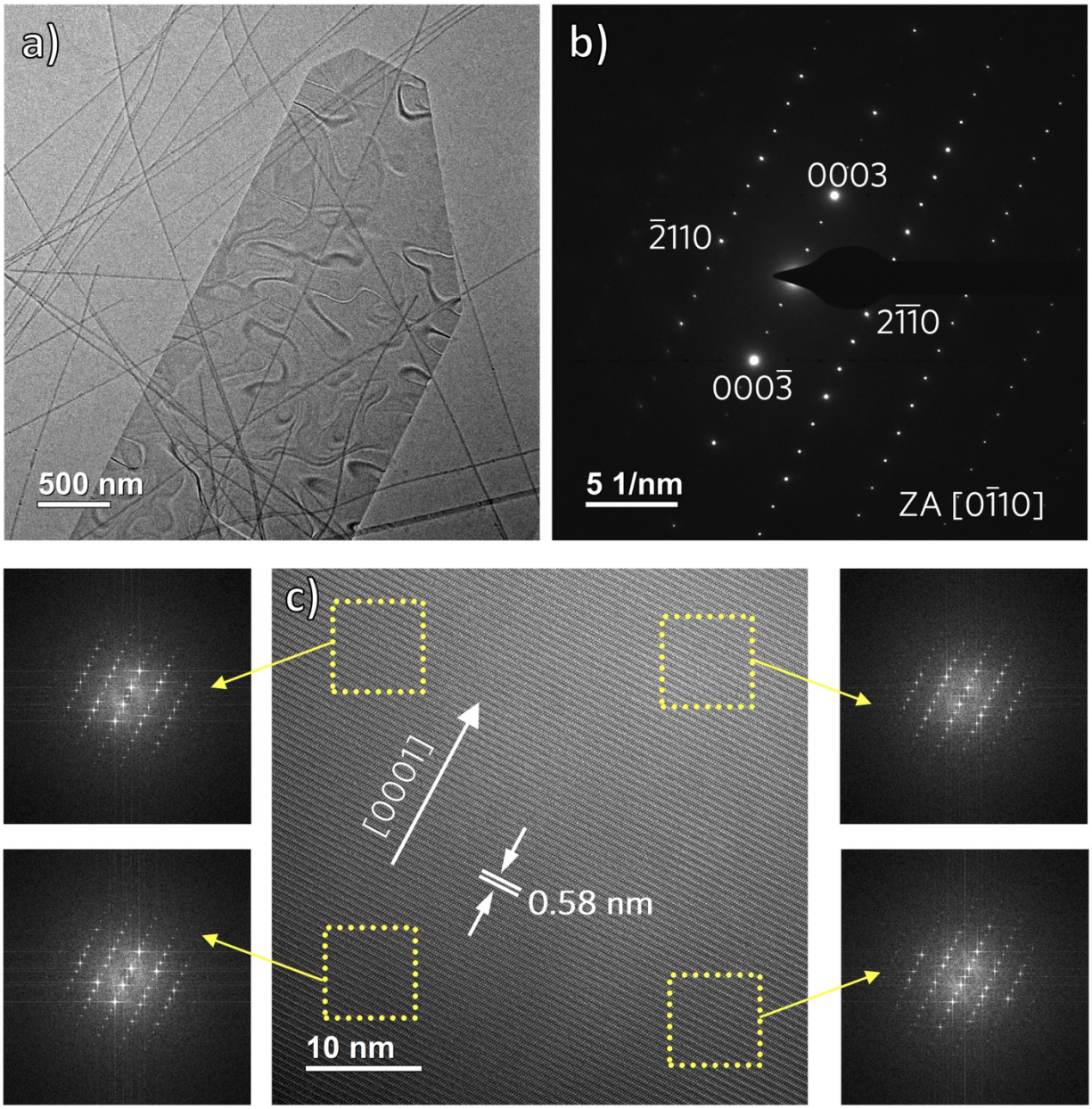

Supplementary Figure 1. (a) TEM image of Te nanoplate. Some nanowires are also found near the sample. (b) SAED pattern of the same area showing a single-crystalline pattern corresponding to a zone axis [$0\bar{1}\bar{1}0$]. (c) HR-TEM image of an area in the Te nanoplate near the edge. There are no significant changes in the FFT patterns of the areas marked with squares. Lattice fringes show mean distance of 0.58 nm in good agreement with the *c* lattice parameter of Te. TEM characterization shows no change in the orientation of Te nanoplates, opposite to what is observed in nanowires.

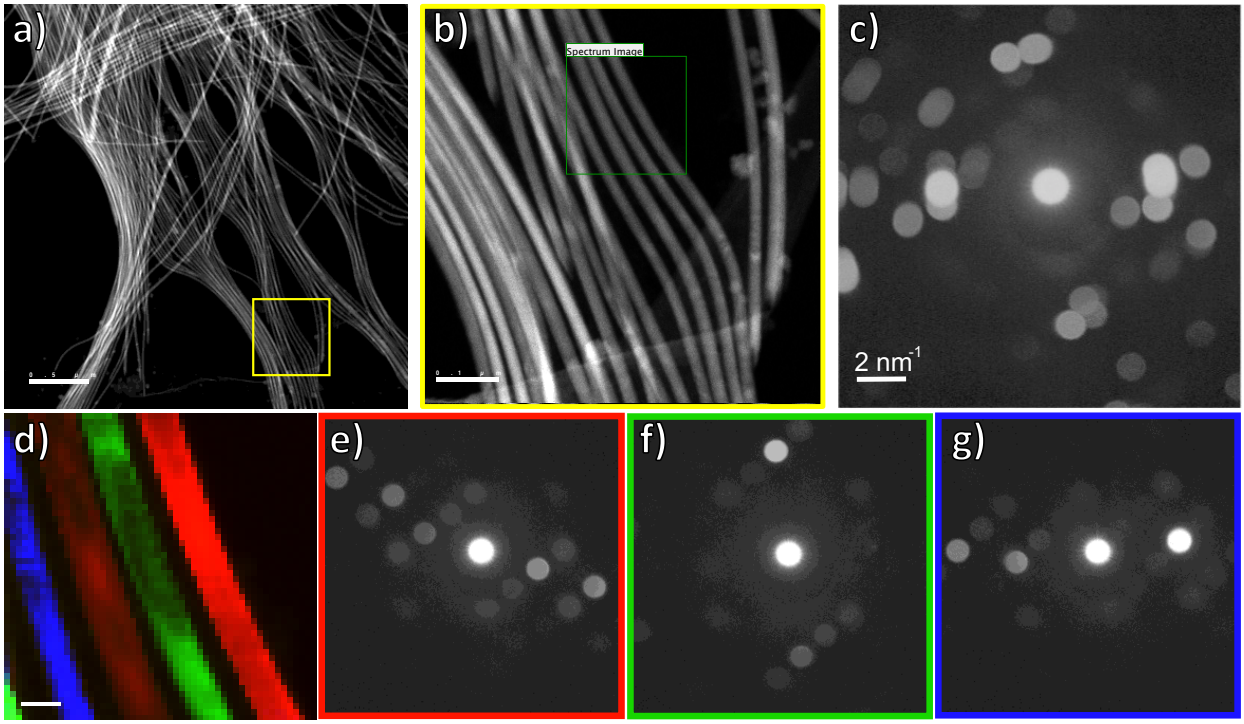

Supplementary Figure 2. (a) HAADF-STEM image of large diameter (16.7 ± 2.0 nm) Te nanostructures, the marked area is shown in (b) from where 4D-STEM data was collected on a 52×51 pixel array with a 3 nm step. (c) Average NBED pattern of the area marked in (b). (d) Reconstructed color-categorized image. Each color represents a class of common diffraction patterns with its representative NBED pattern shown in (e-g).

Orientation imaging microscopy (OIM) techniques, which include TKD, often require processing of the raw signals to yield indexable Kikuchi diffraction patterns that allow for the rapid identification of microstructural orientation. A dataset averaged static background subtract is commonly used to eliminate variations in intensity caused by various scattering phenomena that are not orientation specific. In order to successfully index a reasonable number of the low signal-to-noise TKD patterns, advanced post-processing was required. Nearest neighbor averaging was employed to help increase the S:N, dynamic background subtraction and division helped account for the variable diffuse scattering caused by the sample's constantly varying thickness, and a median smoothing filter further decreased Poisson noise. These techniques do slightly degrade both the spatial and orientation resolutions, however, combined they overcome the poor S:N ratio and yield indexable patterns. **Supplementary Figure 3** shows TKD OIM data from a bundle of Te nanowires. The TKD data from these wires was significantly fainter than from the Te nanoplates, (c) and (g) are TKD patterns after standard post-processing showing faint orientation signal. The advanced post-processing strategies discussed above were used to accentuate the faint signals yielding indexable data. The post-processed patterns shown in (d–f) are from the top, center, and bottom of the red nanowire highlighted by the red arrow where each position is marked with a symbol; the patterns shown in (h–j) are from the top, center, and bottom of the green nanowire marked with green arrow. Each of these shows small orientation changes across the length of the nanowire. There are some nanowires which appear to exhibit multiple orientations along their length, however upon closer inspection these orientation changes are virtually non-existent. The patterns shown in (c–j) are all from the centers of the nanowires where the beam interaction volume was greatest, the faint signal faded as the beam moved away from the full-thickness of the nanowire. The TKD presented shows that these nanowires do not appear to exhibit the chirality of interest in this manuscript, this is expected as this is only found in the smallest nanowires we have investigated. The faint signals present in thick nanowires required significant effort to index, signals from smaller nanowires (*i.e.,* nanowires expected to have a chiral nature) were unable to mapped to orientation space. Thus, 4D-STEM appears to be the only method with which we can directly observe the chirality of Te nanowires.

TKD from ~30 nm thick Te nanoplates is shown in Supplementary Figure 4. The patterns collected were often indexable using standard processing (*i.e.,* a static background subtraction). By employing the more advanced processing a significantly higher fraction of the nanoplate was

indexed and the resultant IPF, (b), shows the nanoplate to be of a single-grain character across its extent. Note that the apparent grain boundary of the pink grain highlighted by arrows at the left-hand-side is an artefact of the orientation space mapping onto the IPF. (d) and (e) show patterns from on either side of the boundary. Unindexable regions are present but these are often associated with varying thickness of the carbon support film and/or Te nanowires crossing both above and below the nanoplate, as seen in (a).

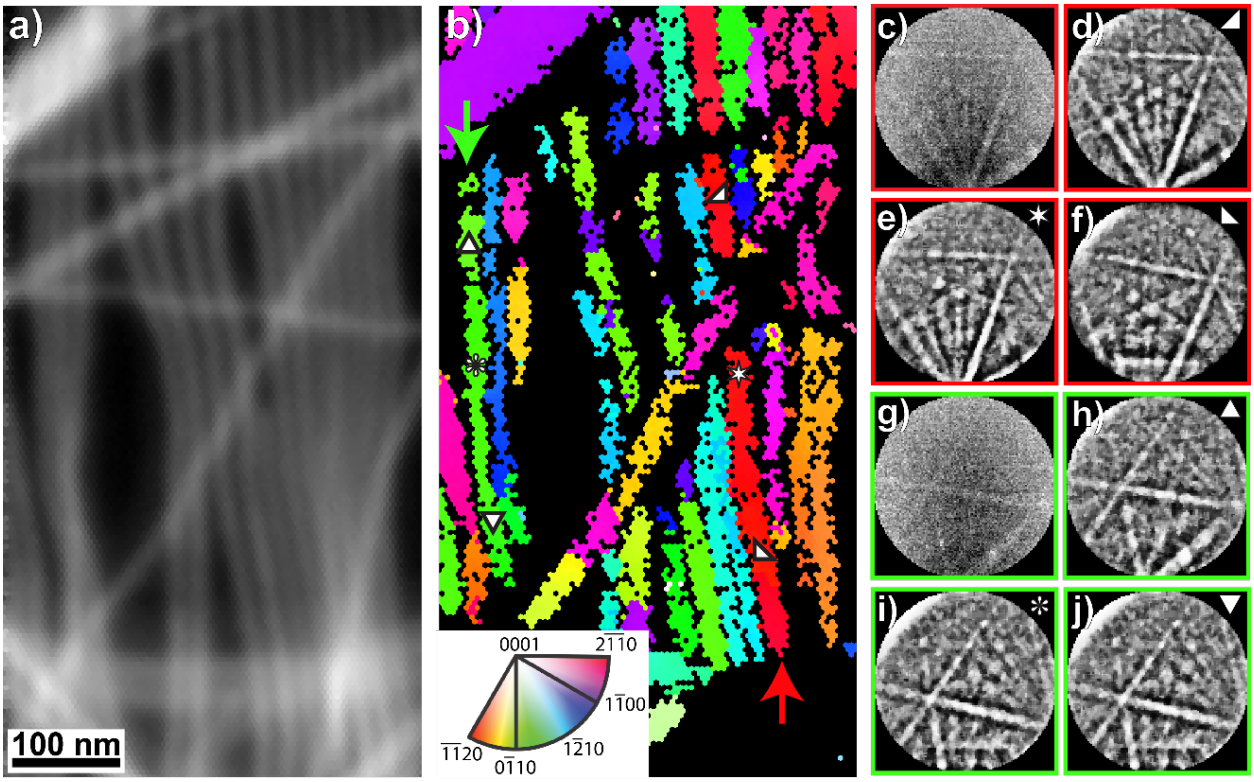

Supplementary Figure 3. (a) A secondary electron micrograph of a bundle of relatively large diameter Te nanowires. (b) An inverse pole figure (IPF) showing nanowires all maintaining *virtually* the same orientation along their respective lengths. (c) & (g) TKD patterns after static background subtraction from the top of the red and green nanowires (arrowed) showing faint orientation signal. (d) & (h) The same TKD patterns shown in (c) & (g) after significant post-processing. (e) and (f) TKD patterns from the center and bottom portions of the red wire and (i) and (j) from the green wire, each showing very small changes in orientation along the length of the nanowires.

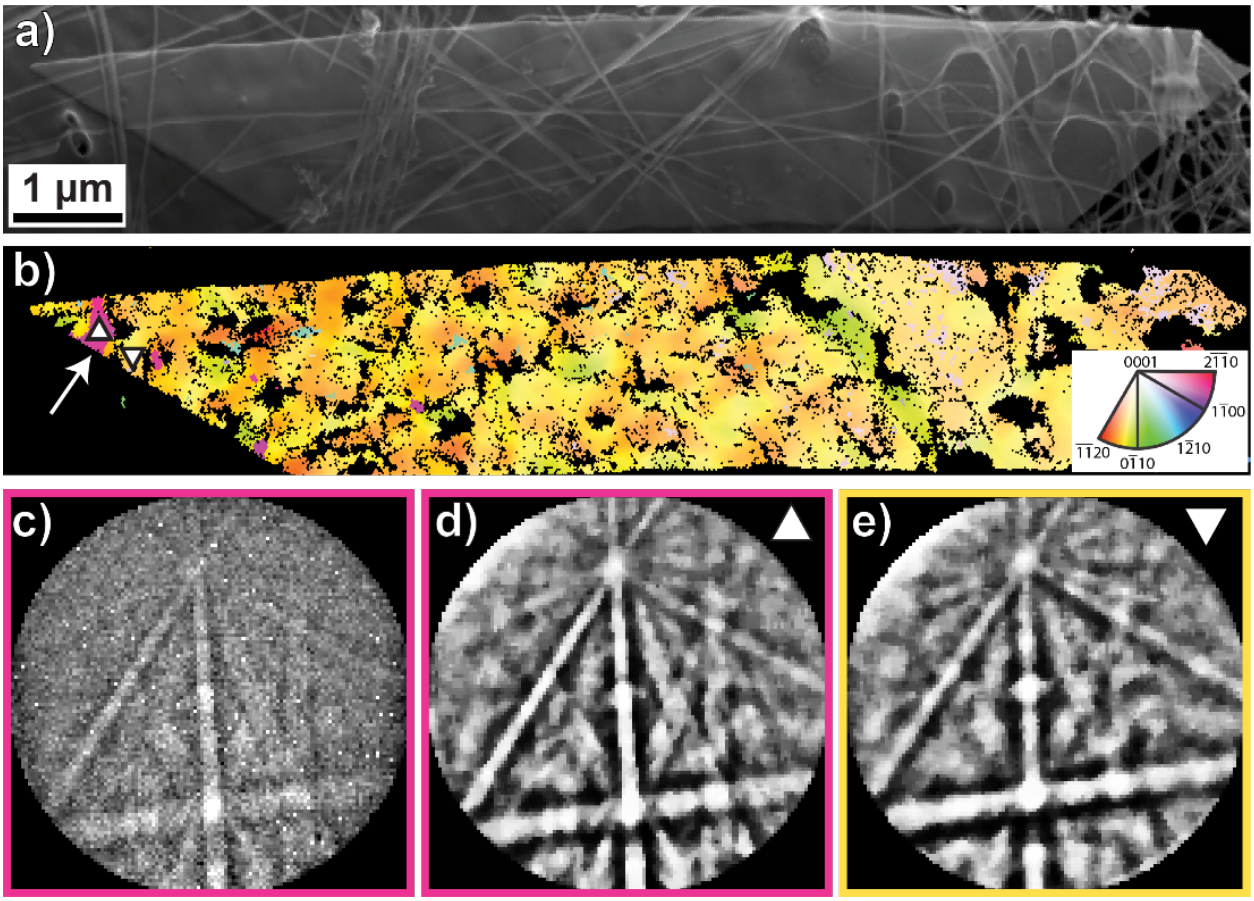

Supplementary Figure 4. A secondary electron micrograph of the Te nanoplate from which TKD data was collected. (b) IPF showing the single-orientation character of the nanoplate, arrows highlight a discontinuity in the orientation color scheme that falsely appears as a crystallographic change. (c) A TKD pattern collected from the pink region in (b) showing an as collected pattern with a static background subtraction. (d) The same TKD pattern shown in (c) with advanced post-processing to reveal full orientation data. (e) A TKD pattern from just across the apparent orientation change showing virtually the same orientation as found in (d).

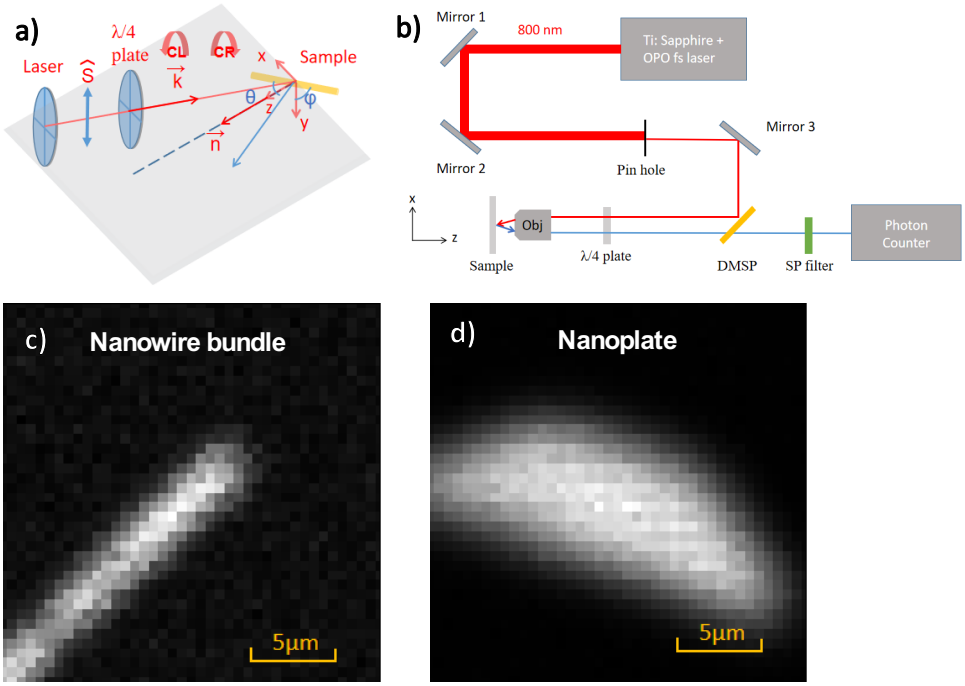

Supplementary Figure 5. (a) The nonlinear optical circular dichroism (CD) of tellurium nanowires (NWs) observed through second-harmonic generation (SHG). Circularly polarized 800-nm pulses were focused onto the sample with a spot size of about 2 μm. The incident angle θ is centered at 10° with respect to the normal vector of the sample plane. The angle φ is defined as the angle between the *c*-axis of the NW and the normal vector of the plane in which light propagates. (b) Schematic of the SHG experimental setup. The incident angle of pump light is selected by a pinhole before the objective's back aperture (DMSP: dichroic mirror beam splitter, SP: short pass filter). Scanning SHG micrographs of the (c) chiral nanowire and (d) structurally achiral nanoplate whose SHG response is shown in Figure 5a,b of the main text, respectively. Despite that the chiral space group of Te atomic lattice can also contribute to SHG-CD, the plates have a fixed orientation with the weakest SHG-CD for small incident angle. According to the crystalline symmetry, single-crystal wires oriented with the $[2\bar{1}\bar{1}0]$ direction normal to the substrate shall exhibit SHG-CD approximately proportional to $(\chi_{14}\cdot\sin\Delta\cdot\sin^2\phi)/\chi_{11}$; single-crystal plates with $[10\bar{1}0]$ direction normal to the substrate shall exhibit SHG-CD approximately proportional to $(\chi_{14}\cdot\sin\Delta\cdot\sin\theta\cdot\sin\phi)/\chi_{11}$. Here Δ is the phase difference between χ_{11} and χ_{14}. It is also possible that the Te plate contains both left- and right-handed domains, which cannot be distinguished from diffraction, and have only short-range chirality even for apparent single crystals.